

# SIMULATION OF BUCKLING BEHAVIOR OF ELASTIC STRUCTURES BY APPLIED ELEMENT METHOD

## 応用要素法による弾性構造体の座屈挙動のシミュレーション

Kimiro MEGURO<sup>1</sup> and Hatem TAGEL-DIN<sup>2</sup>

<sup>1</sup> Member of JSCE, Dr. of Eng., Associate Professor, International Center for Disaster-Mitigation Engineering (INCEDE), Institute of Industrial Science, The University of Tokyo (4-6-1 Komaba, Meguro-ku, Tokyo 153-8505, Japan)

<sup>2</sup> Member of JSCE, Ph.D., Lecturer, Cairo University, Egypt

本研究は、著者らが開発を進めている新しい非線形構造解析手法(応用要素法: AEM)を弾性材料の座屈挙動の解析に適用するための理論とそれを用いた解析結果の紹介である。AEM は有限要素法(FEM)の解析精度と拡張個別要素法(EDEM)の適用性を合わせ持ち、それぞれの欠点を補う可能性を有する手法である。従来は主にクラックの発生や進行性破壊現象のシミュレーションを取り上げてきたが、ここでは幾何学的な不安定現象である座屈を対象に、AEMの適用性と可能性を検討してみる。今回提案する新しい理論は定式化が簡単で汎用性の高いために、様々な形状や材料から構成される構造物に適用可能である。この手法を用いた解析結果から、AEM が座屈荷重や座屈モード、さらに座屈後の不安定挙動を非常に高い精度で解析できることが確認された。

**Key words:** *Applied Element Method, AEM, buckling, post-buckling behavior, large deformation, computer simulation*

## 1. INTRODUCTION

We have been developing a new method, termed Applied Element Method (AEM), to simulate total behavior of structures from elastic to highly nonlinear behavior including failure process. With this method, various nonlinear behaviors, such as material nonlinear behavior, collapse process with separation and recontact between elements can be simulated accurately with reasonable CPU time. Complicated material modeling and special knowledge on location and/or direction of cracks is not necessary before the analysis.

The AEM assumes virtual discretization of structural members. Each element totally represents stresses, strains, deformations and failure of a certain area. The accuracy of the method in small deformation range including Poisson's ratio effect was checked in Refs. (1), (2), and (3). Non-linear behavior such as crack initiation, propagation and opening and closing of cracks during cyclic loading are investigated in Refs. (2) and (3). Since the failure criteria is based on the principal stresses of the material, element shape and discretization pattern will not effect the simulation results unlike the Extended Distinct Element Method, EDEM,<sup>4)</sup> and the Rigid Body Spring Model, RBSM,<sup>5)</sup> whose simulation results heavily depend on the element shape and discretization.

Although our final goal is to simulate the collapse process of the structure accurately for reducing human

causalties due to earthquake, before discussing the collapse behavior, accuracy of this method would be verified in large deformation range. This paper introduces a numerical technique capable to follow the large deformation behavior of structures. Unlike the FEM, there is no need to formulate the geometrical stiffness matrix and this makes the method general and it can be applied for any case of loading or structure type. Accuracy of the proposed new technique is discussed by comparing the numerical analysis results with the theoretical results.

## 2. SIMULATION OF BUCKLING AND POST BUCKLING BEHAVIOR IN STATIC CONDITION

The formulation presented in Ref. (1) cannot be used to study large-scale deformation because only the material non-linearity is taken into account and not the geometric non-linearity. To account for these geometrical changes, a simple numerical procedure is introduced. The main assumption in the formulation is that the direction of applied forces does not change during the analysis. The general equilibrium equation is

$$[K][\Delta U] = \Delta f + R_m + R_G \quad (1)$$

where  $[K]$  is nonlinear stiffness matrix;  $\Delta f$  the incremental applied load vector and  $[\Delta U]$  the incremental displacement vector. The terms,  $R_m$  and

$R_G$  are residual force vectors due to material and geometrical non-linearity respectively.

The method is implemented by assuming the zero initial values for  $R_m$  and  $R_G$  and then the equation is solved to get incremental displacement,  $[\Delta U]$ . Structure geometry is modified according to calculated incremental displacements. Spring force vectors are modified according to the new element configuration. With these geometrical changes incompatibility occurs between applied forces and internal stresses. Then check the situation of cracking and calculate the material residuals load vector  $R_m$  (In elastic analysis,  $R_m$  equals zero). Calculate the element force vector,  $F_m$ , from surrounding springs of each element. And then calculate the geometrical residuals around each element from the equation below.

$$R_G = f - F_m \quad (2)$$

Equation above means that the geometrical residuals account for the incompatibility between external applied forces,  $f$ , and internal forces,  $F_m$ , due to modification of geometry of the structure. Calculate the stiffness matrix for the structure in the new configuration considering stiffness changes at each spring location due to cracking or yield of reinforcement. Then apply again a new load or displacement increment and repeat the whole procedure. Residuals calculated from the previous increment can be incorporated in solution of Eq. (1) to reduce the time of calculation.

Although this technique is simple, the numerical results showed high accuracy in following the structural behavior. However, the following limitations were encountered:

1. Complete symmetry of the structure and loading should be avoided during the large deformation analysis.
2. It should be emphasized that small deformation theory is assumed during each increment.

### 3. NUMERICAL ANALYSIS & RESULTS

#### (a) Fixed Base Cantilever

The first case study is performed using a fixed base elastic cantilever under axial load. The height of the member is 12.0 m and the cross section is 1.0 m x 1.0 m. The Young's modulus assumed is  $8.4 \times 10^4$  tf/m<sup>2</sup>. The load is applied at the top of the column with the constant-rate vertical displacement. To break symmetry of the system, the stiffness of one of edge elements was increased by just 1% relative to the other elements. **Figure 1** illustrates the deformed shape of the cantilever during and after buckling. **Figure 2** shows the horizontal and vertical displacements at the loading point in three different cases with and without

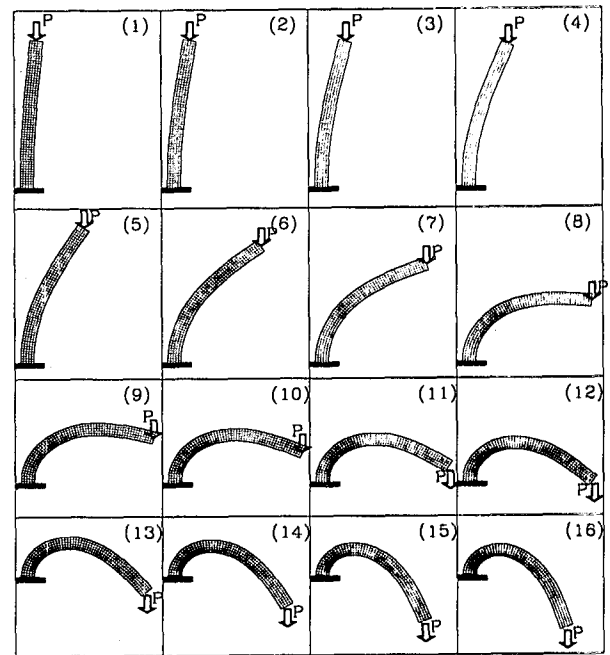


Fig. 1 Post buckling behavior of a cantilever

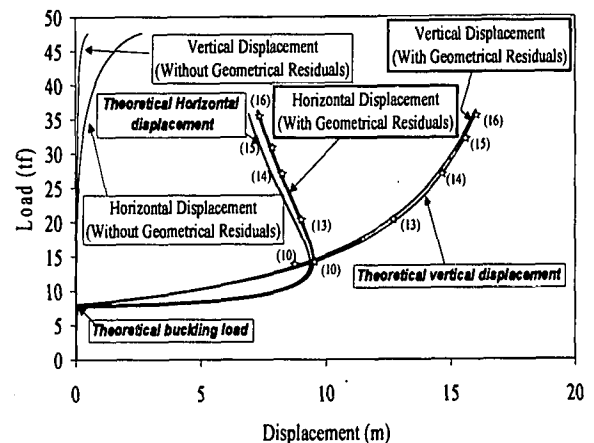


Fig. 2 Post buckling behavior of a cantilever

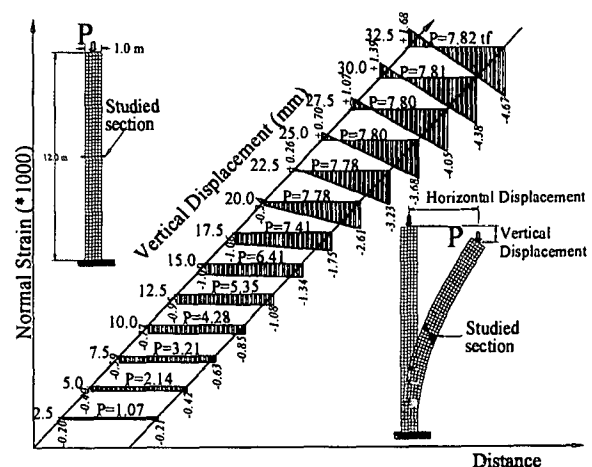


Fig. 3 Variation of internal stress distribution during buckling

consideration of the geometrical residuals together with the theoretical load-displacement relations<sup>6</sup>. The theoretical results can be obtained by the following procedure:

1. Assume the angle  $\alpha$  (ranges between 0 and  $\pi$ ).
2. Solve Eq. (3) below numerically and calculate the applied load. Where  $P$  is the applied load;  $E$  Young's modulus;  $I$  moment of inertia;  $L$  the cantilever length and  $\Phi$  the integration parameter.

$$P = \frac{EI}{L^2} \left[ \int_0^{\frac{\pi}{2}} \frac{d\Phi}{\sqrt{1 - \sin^2\left(\frac{\alpha}{2}\right) \sin^2(\Phi)}} \right]^2 \quad (3)$$

3. Calculate the horizontal and vertical displacements. And then assume a new angle  $\alpha$  and go to the step (2).

In theoretical results, the effects of axial and shear deformations are neglected. Although these effects are relatively small, they are taken into account in our analysis. From Figs. 1 and 2 the following can be noticed:

1. The load-displacement relation obtained when the geometrical residuals are considered is close to the theoretical values till very large displacements.
2. The calculated buckling load without consideration of geometrical residuals, only with modification of geometry, was about 47 tf which is quite larger than the theoretical one (7.8 tf). This means that modification of the geometry only during the analysis is not sufficient.
3. The calculated load-displacement relation is tangent to the horizontal line at the buckling load value which agrees well with the theory.
4. Slight increase in the load after buckling results in very large displacements.
5. When the vertical displacement is about 9 m, horizontal displacement begins to decrease.
6. The cantilever shape changes after buckling to an arch, which makes the stiffness of the specimen increase after buckling.

Changes in internal stresses of an intermediate section during analysis are shown in Fig. 3. Before buckling, stresses are mainly uniform compression and only axial deformations are observed. After reaching the buckling load, although the applied load is constant ( $P \approx 7.8$  tf), bending moments generates and large deformation occurs because of the buckling bending moments. This shows one of the strong points in our analysis that mechanical behavior of any point in the structure can be followed accurately even if large deformations occur.

## (b) Snap Through Buckling of Two-Member Truss

The second case study is a simulation of buckling behavior of two-member truss. The truss dimensions and loading point are shown in Fig. 4. The Young's modulus is assumed  $2.1 \times 10^4$  t/m<sup>2</sup>. Half of the truss is analyzed because of symmetry. The analysis was performed by controlling the displacement at intermediate hinge. The load-displacement relation and the member force are shown in Fig. 4. The results of the load-displacement are compared with the theoretical ones.

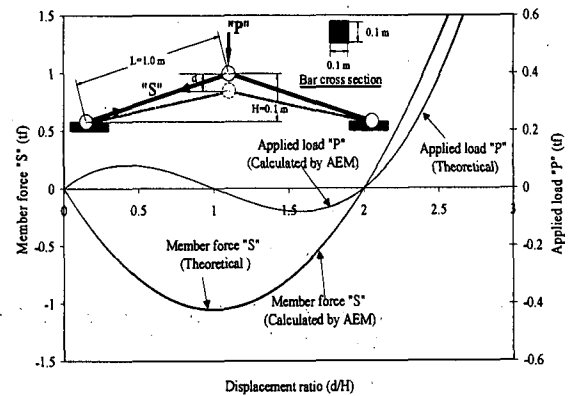


Fig. 4 Relations between applied load, member force and displacement ratio under vertical constant rate applied displacement condition

Almost no difference exists between the calculated and theoretical results. The truss during deformation passes through the following stages:

1. Because the member length decreases during loading, compressive member force increases. The shortest member length, maximum member force, is achieved when the member becomes horizontal.
2. When the member is horizontal, compression force is maximum while the applied load value is zero since it is applied in vertical direction.
3. Increasing the displacements after horizontal position leads to increase the member length, and hence, compressive force is released. The direction of applied load is reversed.
4. When  $(d/H)$  value equals 2.0, the member length becomes the same as the initial value and hence, member force and applied load become zero.
5. Increasing the applied displacement leads to increasing the tension force in the members.

## (c) Elastic Frame with Fixed Support Conditions

The third case study is a simulation of buckling of elastic frame with fixed base. The frame cross section is 0.5 m x 0.5 m. Modulus of elasticity is assumed  $2.1 \times 10^4$  tf/m<sup>2</sup>. The frame dimensions and loading points are shown in Fig. 5. The load is applied at constant-rate. To break symmetry of the system, the stiffness of one of edge elements was increased by just 1 %

relative to the other elements. This analysis cannot be performed under displacement control because displacement of frame corners after buckling are different because of change in values of axial force in the columns. Making the analysis under load control necessitates that the applied load increment should be very small after buckling.

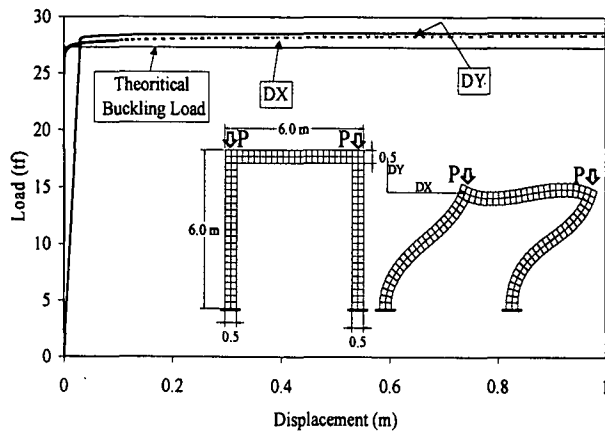


Fig. 5 Load-deformation relation of a fixed-fixed frame under vertical loads. (Side sway is permitted.)

The results are shown in Fig. 5. It can be noticed that the buckling load obtained is very close to the theoretical one<sup>6)</sup>. After buckling, displacements increase drastically in few increments because the loading is applied under load control.

#### 4. CONCLUSIONS

A new extension to AEM for studying the large-scale geometrical changes is introduced in this paper. It was proved through numerical simulations that this technique has the following advantages:

1. Simple compared to the other existing numerical methods.
2. Structural behavior can be accurately followed even in large deformation range. The simulated buckling loads, buckling modes and internal stresses agree well with the theoretical results.
3. Since the technique is general, it can be applied to any structure or material type.
4. This technique can be easily extended to follow the complete collapse process of structures.

However, there are some limitations in the application of this method:

1. Since the load direction is assumed constant, follower loading condition, which means that applied load direction changes when the member buckles, and non-conservative loads in general cannot be studied using the proposed formulation.
2. Although the applied load condition can be adopted as load and displacement control, both of them have their own limitations. Load control can not follow post peak behavior while displacement control technique can not follow cases when the tangent to the load-deformation curve tends to be vertical<sup>1)</sup>. In addition displacement control technique cannot be adopted to cases where load is applied at many points. However, the method can be extended easily to follow other methods of loading like energy control or arc length control methods<sup>6)</sup>.

#### REFERENCES

1. Kimiro Meguro and Hatem Tagel-Din: Development and application of a new model for fracture behavior analysis of structures, Proc. of the Workshop on Earthquake Engineering Frontiers in Transportation Facilities, Post-Earthquake Reconstruction Strategies: NCEER-INCEDE Center-to-Center Project, Technical Report NCEER-97-0005/INCEDE Report No.1997-01, pp.265-279, 1997.10.
2. Kimiro Meguro and Hatem Tagel-Din: A New Simplified and Efficient Technique for Fracture Behavior Analysis of Concrete Structures, Proceedings of the Third International Conference on Fracture Mechanics of Concrete and Concrete Structures (FRAMCOS-3), Vol. 2, pp. 911-920, Gifu, Japan, 1998.10.
3. Kimiro Meguro and Hatem Tagel-Din: A new efficient model for fracture analysis of structures, Proceedings of 16th annual Conference on Natural Disaster Science, Osaka, Japan, Oct. 1997.
4. Kimiro Meguro and Motohiko Hakuno: Application of the extended distinct element method for collapse simulation of a double-deck bridge, Structural Eng./Earthquake Eng., Vol. 10. No. 4, 175s-185s., Japan Society of Civil Engineers, 1994.
5. Tadahiko Kawai: Some considerations on the finite element method, Int. J. for Numerical Methods in Engineering, Vol. 16, pp. 81-120, 1980.
6. Timoshenko S. and Gere J.: Theory of elastic stability, McGraw-Hill Inc., 1961.